European Geosciences Union General Assembly 2011
Vienna, Austria, 4-9 April 2010
Session NP6.3 : Turbulence in the atmosphere

Hurst-Kolmogorov dynamics applied to temperature fields for small turbulence scales

P. Dimitriadis, P. Papanicolaou and D. Koutsoyiannis

Department of Water Resources and Environmental Engineering
National Technical University of Athens

(www.itia.ntua.gr)

1. Abstract

Two-dimensional (2D) spatio-temporal temperature records obtained from tracer concentration measurements on the plane of symmetry of heated jets (small turbulence scale) are statistically analyzed and the presence of Hurst-Kolmogorov (HK) dynamics is detected. The 2D HK process is then fitted to the data and synthetic time-varying and/or spatial fields are generated for temperature, which are consistent with the observed. Moreover, the 2D HK process is formulated assuming anisotropy, so as to take into account possibly different autocorrelation decay rates (Hurst coefficients) in each dimension of the field.

2. Hurst phenomenon and the HK process

"*High tendency of high/low values to occur in natural events*": Hurst (1951) ➔ Slowly decaying autocorrelation over scale➔ Power-law behaviour (Kolmogorov, 1940).

$$\left(\underline{Z}_v^{(k)} - \mu\right) =_d \left(\frac{k}{l}\right)^A \left(\underline{Z}_v^{(l)} - \mu\right), \text{ where } \mu = E[\underline{Z}_v], A = D(1 - H), \underline{Z}_v^{(k)} = \frac{1}{k^D} \sum_{i_1=(v_1-1)k+1}^{v_1 k} \cdots \sum_{i_D=(v_D-1)k}^{v_D k} \underline{Z}_{i_1,\ldots,i_D}$$

- $\underline{Z}$: random field of interest (assumed stationary and isotropic)
- $\underline{Z}_v$: mean aggregated field (at a spatio-temporal scale)
- v: vector index of random field indicating location in the field
- k,l: any aggregation scales of the process
- μ: mean of the process
- $=_d$: equal in distribution function
- A: power law exponent of autocorrelation over scale
- D: dimension of vector index space of random field (v)

3. Hurst coefficient (H) and autocorrelation function (ρ) of the HK process

• HK process depends on the characteristic parameter $0<H<1$. Here, the estimation of the H coefficient is done via the minimization of the square error (SE_H) of the empirical $(S^{(k)})^2$ and true ($\gamma^{(k)}$) variance over scale k of the process, a method by Tyralis and Koutsoyiannis (2010).

$$SE_H = \sum_{k=1}^{k'} \left[2\ln(\tilde{S}^{(k)}) - \ln(\gamma^{(k)}) \right]^2 / k^p,\ p = 2,\quad E\left[\left(\tilde{S}^{(k)} \right)^2 \right] = R\left(S^{(k)} \right)^2,\quad R(k;H) = \frac{N/k^D - 1}{N/k^D - \left(N/k^D \right)^{2H-1}}$$

• The autocovariance γ (acvf) and autocorrelation function ρ (acrf) of the HK are expressed as:

$$\gamma_{c(0)}^{(k)} = k^{-B}\gamma_{(0)}^{(1)} \text{ and } \gamma_{(r)}^{(k)} = L_D r^{-B} \qquad \text{where } B = 2D(1-H) = 2A$$

$$\rho_{c(r)}^{(k)} = \gamma_{(r)}^{(k)} / \gamma_{(0)}^{(k)} \rightarrow \rho_{c(r)} = L_D r^{-B} / \gamma_{(0)}$$

c stands for continuous

L_D is a coefficient

r is the lag

- $0 < H < 0.5 \rightarrow$ Anticorrelated ($\rho < 0$)
- $H = 0.5 \rightarrow$ Independent ($\rho = 0$)
- $0.5 < H < 1 \rightarrow$ Correlated ($\rho > 0$)

Note: The continuous acvf and acrf become infinite for scale 0 and lag 0, respectively.

4. Field Normalization

HK process generates random fields that follow the $N(0,1)$. Here the following transformation (Papalexiou et al., 2007) is used, where its coefficients p_i are estimated through the minimization of the square error of the transformed data and the $N(0,1)$ distribution function.

$$Z_N = \left(p_1 Z^{-p_5} + p_2 \right) \left(p_3 + \sqrt{(1+1/p_4)\ln\left[p_4 \left(Z - p_3 \right)^2 + 1 \right]} \right)$$

5. Discrete autocorrelation function of the HK process

For the discrete acrf, one can adapt the Koutsoyiannis et al. (2010) approximate solution (KAS)

$$I_{D,r} = \frac{\rho_{discete}(j_1,\ldots,j_D)}{L_D}\gamma_{(0)} = 2^D \int_{v_1=0}^{1} \ldots \int_{v_D=0}^{1} \left[(j_1^{\,2} + \ldots + j_D^{\,2}\right]^{-B/2} \left[\left(1-\left|j_1\right|\right)\ldots\left(1-\left|j_D\right|\right)\right] dv_1 \ldots dv_D,\ r = \sqrt{j_1^{\,2} + \ldots + j_D^{\,2}},\ j_i \in \mathbb{N}$$

$$\varrho_{\text{discete}}(r) = \rho_{D,r} \approx \min\left\{C_D\left(\rho_{1,r}/C_1\right)^D, \rho_{1,r}\right\}\text{: KAS}\ ,\ \rho_{1,r} = \left|r+1\right|^{2H}/2 + \left|r-1\right|^{2H}/2 - \left|r\right|^{2H}$$

$$I_{D,0} = \frac{\rho_{D,0}}{L_D}\gamma_{(0)} \approx \frac{1}{C_D},\ C_D = \frac{(2H-1)[D(2H-1)+1]}{(D+1)}$$ Note that for great lags: $\rho_{D,r} \approx \frac{C_D}{r^B}$

6. Simulation scheme for generating HK process

SMA stands for Symmetric Moving Average and it can be used to generate a stochastic process with any structure of autocorrelation or power spectrum (Koutsoyiannis, 2000).

$$Z_v = \sum_{y_D=-q}^{q} \ldots \sum_{y_1=-q}^{q} \alpha_y W_{v-y}$$

- Z_v: generated normalized random field of interest
- W: discrete white noise (random field) with zero mean ($\mu_w = 0$) and unit standard deviation ($\sigma_w = 1$) (since $\underline{Z}$ has been normalized).
- q: finite limit for the range of coefficients α_y (for m, the desired number of autocorrelation coefficients that are to be preserved).
- α_y: field of coefficients that can be determined through the Fourier transform F_γ of the autocovariance field γ_Z (Koutsoyiannis, 2000, Koutsoyiannis et al. 2010).

7. Spectral density and α_y coefficients of SMA

The spectral density F_γ of the stochastic field can be determined via the Fourier transform of the discrete form of autocovariance $\gamma_{\text{discrete}}(r)$. It can be shown that the Fourier transform F_α, of the field α_y, is related to F_γ (for $q=\infty$), thus the α_y field can then be estimated.

$$F_\gamma(s) = \frac{(2\pi)^{D/2}}{s^{D/2-1}} \int_0^\infty |r|^{D/2}\, \gamma(r) J_{D/2-1}\{2\pi s r\}\, dr = \frac{(2\pi)^{D/2}}{s^{D/2-1}} L_D \int_0^\infty |r|^{D/2-B}\, J_{D/2-1}\{2\pi s r\}\, dr \rightarrow$$

$$\rightarrow F_\gamma(s) = L_D E |s|^{B-D}, \text{where } E = \pi^{-D/2+B} \frac{\Gamma[(D-B)/2]}{\Gamma[B/2]}, \; for\; 1 < B < D \rightarrow \frac{1}{2} < H < 1 - \frac{1}{2D}, s \in \mathbb{R}$$

$$\text{Thus, it can be shown that, } F_{\gamma_{\text{discete}}} \overset{\text{great lags}}{\approx} C_D \gamma_0 E |s_{discrete}|^{B-D}, \text{ for } \frac{1}{2} < H < 1 - \frac{1}{2D}, s_{\text{discrete}} \in \mathbb{N}$$

$$\text{Also, it can be assumed that, } F_{\gamma_{\text{discrete}}} \approx K_D |s_{\text{discrete}}|^{B-D}, \text{for } 0<H<1 \text{ and } K_D \text{ a coefficient}$$

From the above equations and assumptions it can be derived that:

$$F_\alpha \overset{\text{extension of 1D SMA}}{=} \sqrt{F_{\gamma_{\text{discrete}}}} \rightarrow \alpha_y \approx \alpha_0 \rho(\|y\|; H'), \text{where } B' - D = (B-D)/2 \rightarrow H' = (H+0.5)/2$$

$$\gamma_0 = \sum_{y_D=-q}^{q} \cdots \sum_{y_1=-q}^{q} \alpha_{y_1,\ldots,y_D}{}^2 \rightarrow \alpha_0{}^2 = \gamma_0 \Big/ \sum_{\boldsymbol{y}=\underbrace{-q,-q,\ldots,-q}_{D}}^{q,q,\ldots,q} \rho^2(\|\boldsymbol{y}\|; H') \quad \text{and} \quad \alpha_{0,q=\infty} = \frac{\sqrt{\gamma_0 C_D(H) E(H)}}{C_D(H') E(H')}$$

8. Experimental set-up

The first scale under investigation is the turbulence microscale (order of mm). This scale is usually observed in boundary layers and turbulent shear flows such as turbulent buoyant jets. An experiment is set at the laboratory of Applied Hydraulics of the NTUA by P. Papanicolaou, where measurements are based on the LIF (laser-induced fluorescence) technique.

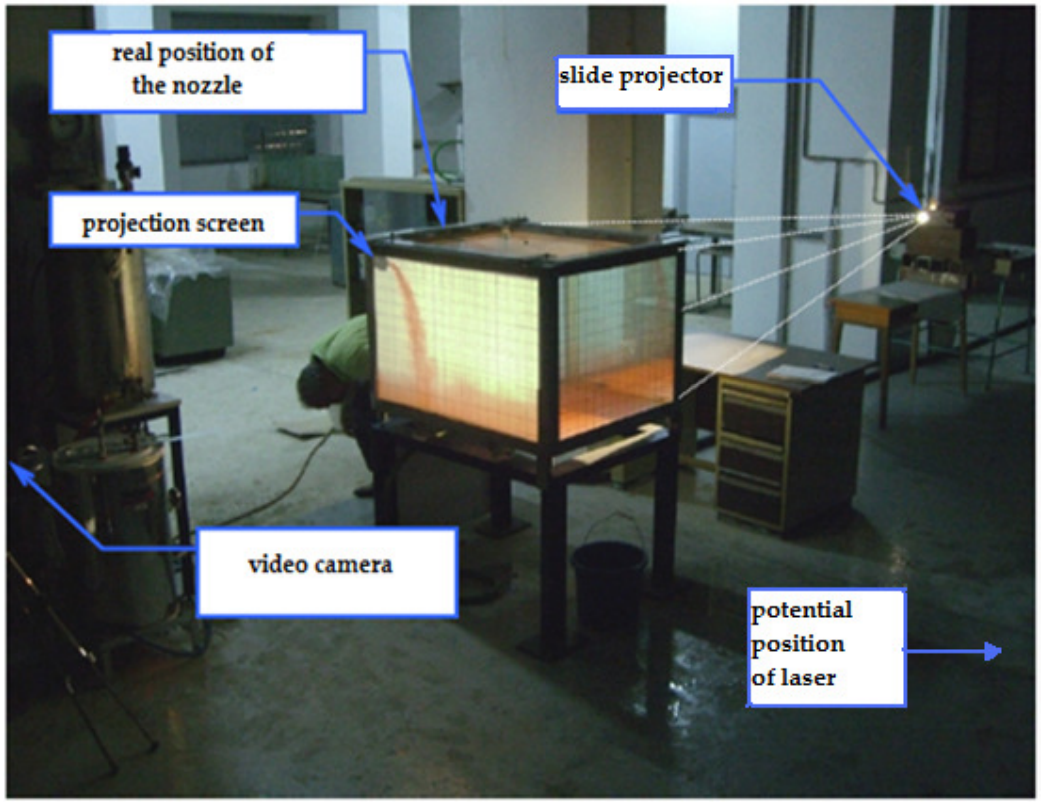

Photograph of the experimental set-up of Turbulent Buoyant Jets (source: Spyridon Michas, PhD on 'Experimental investigation of horizontal, circular and non axis-symmetric buoyant jets, in a homogeneous and stationary environment', supervisor P. Papanicolaou, Department of Civil Engineering, University of Thessaly, 2008).

The buoyant jet is dyed with a rhodamine 6G (R6G) dye with low concentration that does not affect buoyancy. The jet flow field is illuminated with a thin (order of 1 mm) plane sheet of laser light. A DPSS 1 W laser beam at 532 nm (green) is converted to a thin laser light sheet via a rotating prism mirror at 20 kHz. The rhodamine dye excited by the 532 nm wavelength emits (yellow) light at 556 nm. Thus, laser based tomography of the buoyant jet flow-field can be obtained across any desired plane. Then, the experiment is videotaped using a high resolution video-camera pointing normal to the light sheet at 30 frames per second (fps). In this way, the yellow intensity of R6G (measured through the RGB frame format of the camera) can be linked to its concentration (as shown in the next slide).

9. Calibration

- The initial fluorescence light intensity I_o is proportional to the R6G initial concentration C_o if it does not exceed 50 ppm (or μg/L), as shown by Ferrier et al. (1993). Here, this is verified through the measurement of the intensity of several R6G concentrations samples fully mixed into the water-tank, for 2 camera shutter speeds (sp).of 50 and 100 s^{-1}. The 'Ferrier' curves on the graphs are adjusted to the measurements by multiplying with an arbitrary factor as Ferrier et al. (1993) intensity is arbitrary. As the yellow emitted light is formed only by the red and green dye, the blue one will be close to zero. Also, to avoid the influence of the green laser beam, one can link the R6G concentration with the red intensity only.

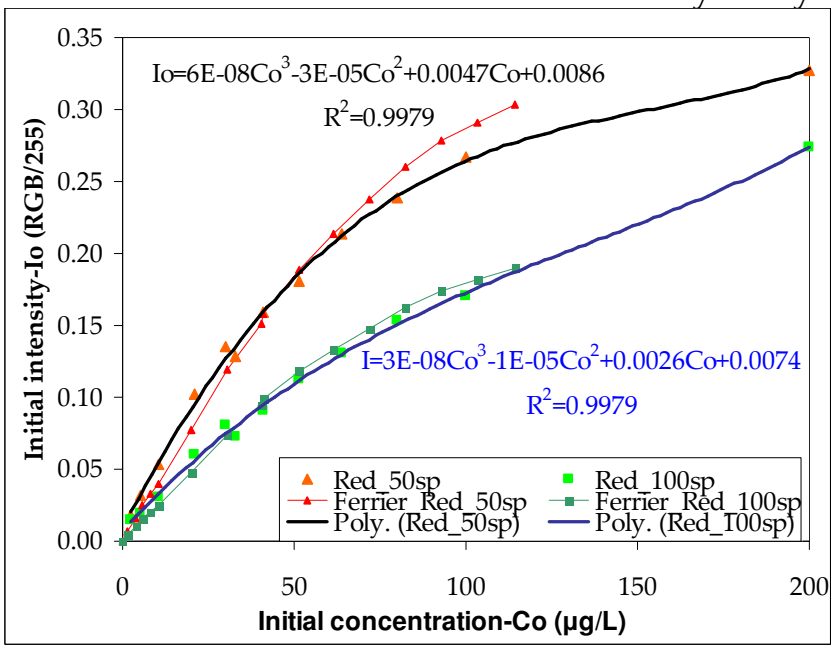

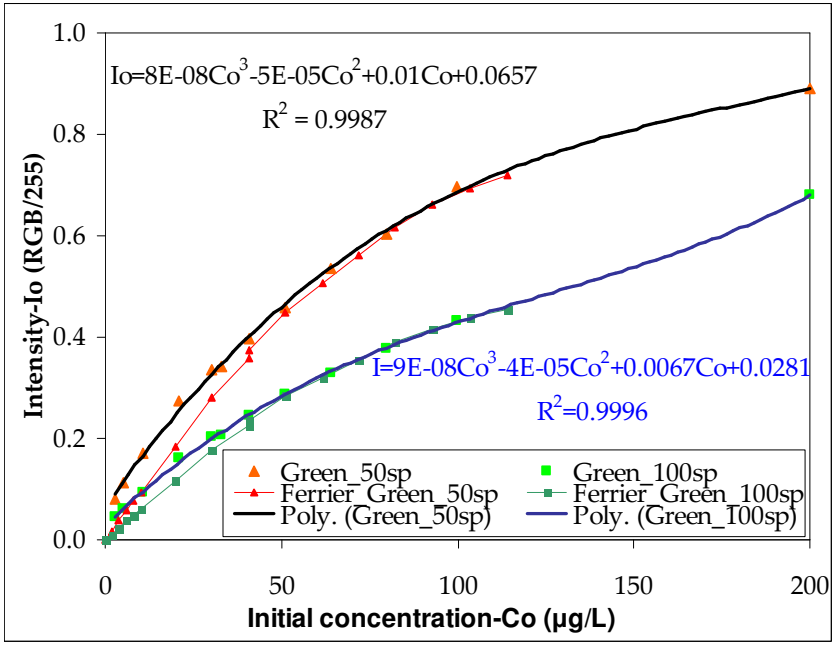

- For concentrations of R6G greater than 50ppm, the attenuation factor can no longer be assumed negligible and it should be accounted for (Ferrier et al., 1993).

$I(x) = I_o e^{-\eta_I x}$, $\eta_I = \eta_{Iw} + \varepsilon_I C$, where η_{Iw} and ε_I are coefficients to be determined experimentally

10. Case study on heated vertical jet

The application presented is based on an experiment of a heated vertical jet held at the laboratory of Hydraulics at the NTUA. By analyzing the video-frames with MATLAB (computer image process program) and using the relationships held on the 'Calibration' slide, one can estimate the color intensity at any point and time of the experiment and thus the spatio-temporal tracer concentration/temperature.

Each frame (2278 in total) corresponds to 1/30 sec and each pixel to approximately 0.048X0.048 cm^2. The grid of the field shown below is 860 x 300 pixels.

Co (μg/l)	SP (Hz)	D (cm)	Q (ml/s)
42.857	100	1.5	15.263
Tjet (oC)	**Tam (oC)**	**M (cm^4/s^2)**	**B(cm^4/s^3)**
29.7	15.6	131.828	48.442
Re	**Im**	**Ri**	**Fo**
1600	5.590	0.238	3.958

D is the nozzle diameter, *Q*, *M*, *B*, F_o, R_i and R_e are the initial discharge, jet specific momentum and buoyancy flux, Froude, Richardson and Reynolds number, T_{amb} and T_{jet} are the ambient and jet temperatures and l_m.the characteristic length scale ($M^{3/4}B^{-1/2}$).

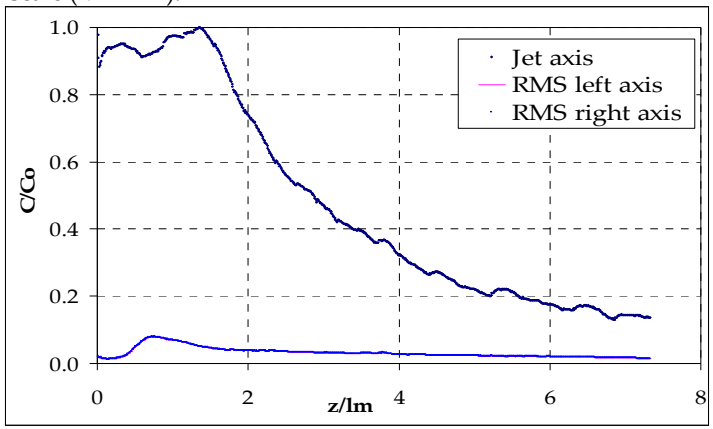

Red intensity (RGB/255) along the averaged jet and RMS axis (left&right RMS axis overlap with each other)

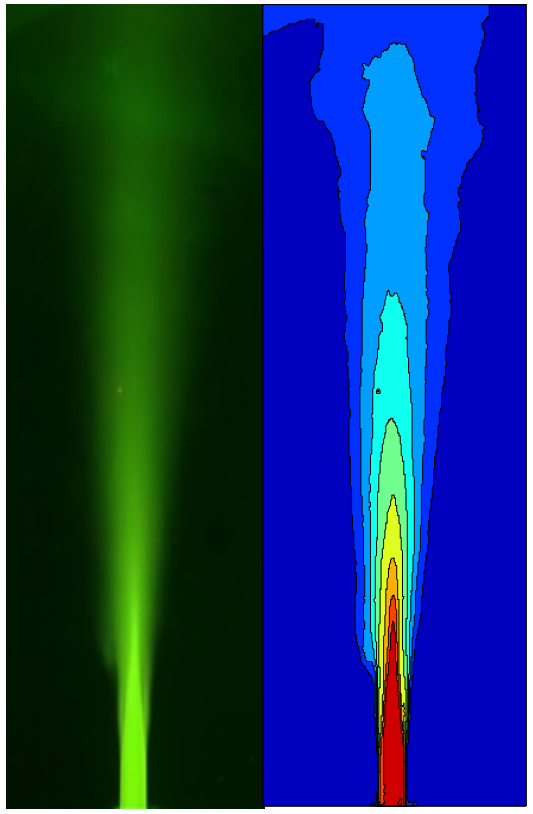

Average of frames (RGB format)

Average of frames (intensity of red)

Standard deviation of frames (RGB format)

Standard deviation of frames (intensity of red)

11. Anisotropy and 2D stochastic simulation model

A separate Hurst coefficient should be assigned to the quantities that are non isotropic to each other. It is still not applicable to create a multi-dimensional model that can synthesize time-series assuming anisotropy (thus assuming a different autocorrelation behavior in each dimension) and that is why scientists tend to use multi-variate models.

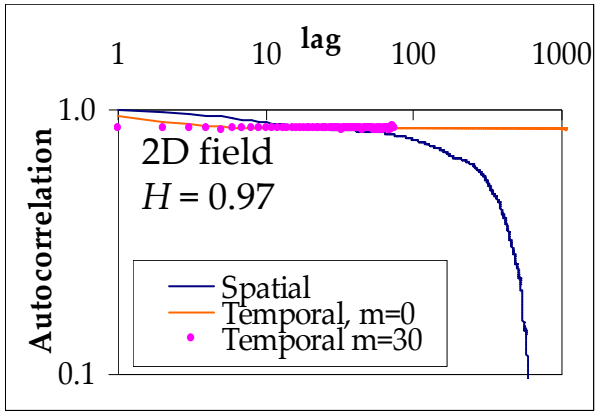

A proposed rough solution would be to omit intermediate data of the field grids, so as the multi-acrfs decay at the same rate (at least for the first lags). So, omitting factor (omfc) m means that the $(m*c)$th cell is omitted in the model, where c is 0,1,…,maximum number of cells in each direction of the sub-field and in the diagonally ones. Here, m is chosen equal to 30, as one can see at the figure on the left, thus the final spatio-temporal grid is 75secondsX860pixels.

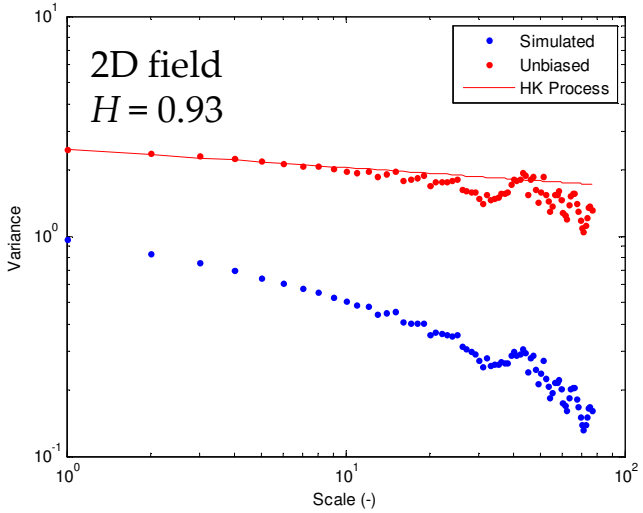

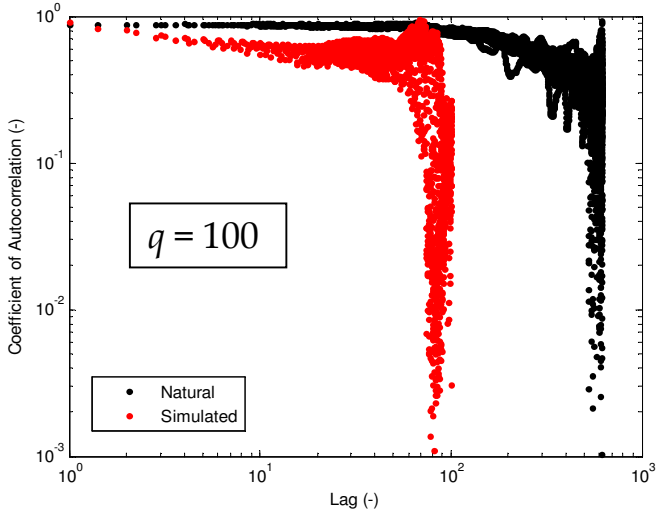

The simulated autocorrelation seems to be smaller than the natural one. This is due to the small q parameter that is chosen, as larger values would enormous increase the numerical simulation time.

12. Conclusions

- A calibration for the LIF technique is performed in order to explore the relationship between the temperature and R6G fluorescence intensity . It is shown that it is linear for R6G concentrations less than 50 μg/L, in agreement with Ferrier et al. (1993). Moreover, it is evident that the red intensity of the RGB color scheme is less sensitive than the green one (which may also be affected by the green laser light intensity), and thus more appropriate to be linked to the temperature concentration.
- A LIF technique is used to visualize a heated vertical jet. Spatio-temporal temperature is estimated through the analysis of the color intensity of the video-frames based on the red intensity of the RGB format. The plane of symmetry of the flow ("jet axis" of the maximum time-averaged temperature) and RMS axis are identified.
- A 2D model is also applied (via the SMA scheme) to generate the observed long-term persistence of temperature along the jet axis. The simulation is done at the plume area (S/l_m>2) of the flow as the observed long-termed persistence is expected away from the nozzle, where buoyancy forces dominate over momentum ones, (M<<B).

References

- Hurst, H.E. (1951) Long term storage capacities of reservoirs. Trans. ASCE 116, 776-808.
- Kolmogorov, A.N., WienerscheSpiralenund einigeandereinteressanteKurvenin HilbertschenRaum, Dokl. Akad. NaukURSS, 26, 115–118, 1940.
- Mandelbrot B. B. (1977), 'The Fractal Geometry of Nature', 248. Freeman, New York, USA.
- Koutsoyiannis, D. (2003), Climate change, the Hurst phenomenon, and hydrological statistics, Hydrological Sciences Journal, 48(1), 3-24.
- Koutsoyiannis et al., (2010), Two-dimensional Hurst-Kolmogorov dynamics and its application to the study of rainfall fields .
- Papanicolaou P.N. and List E.J. (1987). Statistical and spectral properties of tracer concentration in round buoyant jets. Int. J. Heat Mass Transfer, 30(10), 2057-2071.
- PPapalexiou, S.M., A. Montanari, and D. Koutsoyiannis, Scaling properties of fine resolution point rainfall and inferences for its stochastic modelling, European Geosciences Union General Assembly 2007, Geophysical Research Abstracts, Vol. 9, Vienna, 11253, European Geosciences Union, 2007.
- Tyralis H. and D. Koutsoyiannis, Simultaneous estimation of the parameters of the Hurst-Kolmogorov stochastic process, Stochastic Environmental Research & Risk Assessment, DOI: 10.1007/s00477-010-0408-x, 2010.